

Experimental study of performance and prototype of elliptical altitude detection based on global navigation satellite system

Dwi Aji Zulfikar¹, Yoyok Nurkarya¹, Johar Setiyadi¹, Endro Sigit Kurniawan¹, Carudin², Suhadi^{2,3}

¹Hydro Oceanography Study Program, Naval of Technology High School, Jakarta, Indonesia

²Department of Informatics Engineering, Faculty of Information Technology and Digital, Bani Saleh University, Bekasi, Indonesia

³Ministry of Marine Affairs and Fisheries Republic of Indonesia, Jakarta, Indonesia

Article Info

Article history:

Received Mar 16, 2024

Revised Nov 11, 2024

Accepted Nov 20, 2024

Keywords:

Average

Global navigation satellite system

Median

Microcontroller

Mode

Standard deviation

ABSTRACT

Global navigation satellite system (GNSS) is a multi-satellite-based navigation system, in the GNSS positioning process involves several navigation satellites such as global positioning system (GPS) which is a navigation system to bring up more observation data so that it is very useful when determining the desired parameters in a real-time data processing. In the research, an experimental study is used to determine land subsidence which is one of the vertical deformations of the earth's crust as a consequence of crustal dynamics. The result of the analysis is raw position data with the average method of detecting the height of the ellipsoid in the XYZ location area. Data collection is done by observation using the absolute method for one hour for position and fifteen days of observation for height. While the equipment used is u-blox Neo-7M, MCU TTL RS-485 module, ESP32-S Dev Kit V1 module, memory card module and real time clock (RTC). The results of the observation validation analysis are i) GPS-1 Easting 1.09 m and Northing 1.08 m, GPS-2 Easting 1.19 m and Northing 1.32 m, GPS-3 Easting 0.54 m and Northing 0.64 m while GPS-AVG GPS Easting 0.56 m and Northing of 0.64 m, ii) The results of the GPS-1 ellipsoid height analysis are 3.76 m, GPS-2 4.28 m, GPS-3 of 3.69 m, and iii) GPS AVG of 3.01 m.

This is an open access article under the [CC BY-SA](https://creativecommons.org/licenses/by-sa/4.0/) license.



Corresponding Author:

Suhadi

Department of Informatics Engineering, Faculty of Information Technology and Digital, Bani Saleh University

Jl. Madmuin, No. 68 Bekasi Timur, West Java, 17113, Indonesia

Email: hadims71ndl@gmail.com

1. INTRODUCTION

Land subsidence is one of the vertical deformations of the earth's crust as a consequence of crustal dynamics, subsidence changes the vertical position (elevation) of ground control points as reference points for all engineering works and also affects the structure of all infrastructure in other related activities in the area, land subsidence is a major problem faced by several large cities [1]. Observation of land subsidence is needed to see trends in geometric patterns and physical patterns that occur, one of them is the global navigation satellite system (GNSS) survey which is a method of determining point coordinates using satellite technology commonly used in GNSS surveys, namely the global positioning system (GPS). GPS was developed by the United States Department of Defense, apart from GPS positioning with GNSS are GLONASS made by Russia, GALILEO made by Europe, and COMPASS made by China [2]. The development of a national basic framework system that utilizes GPS is continuously operating reference station (CORS). GNSS CORS itself is connected to a web server to facilitate the data retrieval process,

GNSS CORS is an active geodetic frame net in the form of a permanent station (base station) equipped with a receiver and can receive signals from GNSS satellites that operate continuously every day [3]. The core of the technology lies in a network of satellites that continuously emit signals containing precise time and position information, receivers that are usually integrated into devices such as smart phones or vehicle tracking systems, pick up these signals and use trilateration techniques to determine the exact location.

The use of GNSS as a positioning method has been widely utilized, one of which is used for the observation of land movement, basically the use of GNSS for land movement is done by determining the coordinates of monitoring points carefully and periodically. By studying changes in the coordinates of these observation points continuously over time, the speed and direction of movement can be determined. By knowing the velocity and direction of movement, analysis and estimation of the strain can be done [4]. The growth in the number and activities of the population is very high, causing built-up areas including industrial, trade, office, and residential areas, which are a necessity and a means of supporting the activities of the population, this will cause changes in the physical condition of the environment and if not able to control one of the physical impacts that will be faced is a very significant land subsidence [5]. In this study, the use of knowledge gained from the GNSS system for detecting the height of the ellipsoid at XYZ, as well as the efforts made are assembling a prototype GNSS system simply and it is expected that the steps and procedures carried out to develop an equipment that will later be applied to a system in the survey area that requires position observation with more accurate position results and facilitate processing in data management so that it can be used to analyze the needs of developing future survey activities.

Previous research conducted by Fedorchuk [6] was to compare the heights of the global geoid models EGM08, EIGEN-6C4, GECO, and XGM2019e based on the sector analysis obtained relative to the WGS84 and GRS80 ellipsoids to implement the GNSS alignment method in the local area. The global geoid model height determined from the WGS84 ellipsoid should be reduced by 41 cm, the spatial analysis of the geoid model height in the relative system for the northern region shows that the standard deviation of the geoid model height is 13.6 cm, and for the southern region is 36.5 cm. The error of the geoid model height in the relative system is estimated to have a standard deviation of 2.9 cm in the northern region and 2.3 cm in the southern region. The root means square values of the initial errors of the EGM08, EIGEN-6C4, GECO, and XGM2019e models are 8.6, 4.6, 4.4, and 3.8 cm, respectively, and their standard deviation values are 2.0, 2.2, 3.2, and 2.4 cm. This paper also conducted a sectoral analysis of the geoid model error to correct it in the application of the GNSS alignment method within the study area. The standard deviations of the residual errors of the corrected model heights are 1.8, 1.9, 2.5, and 2.0 cm for EGM08, EIGEN-6C4, GECO, and XGM2019e, respectively. The mean square root values of these residual errors for the geoid models are 1.9, 2.0, 2.5, and 2.0 cm.

Previous research conducted by Hamza *et al.* [7] the results of the zero baselines test show that the u-blox multi-frequency receiver, *i.e.*, ZED-F9P, has low noise at the sub-millimeter level. To analyze the impact of the antenna on the obtained coordinates, a short baseline test was applied. Both uncalibrated antennas tested (Tallysman TW3882 and survey) showed satisfactory positioning performance. The Tallysman antenna was more accurate in horizontal positioning, and the difference from the true value was only 0.1 mm; while for the survey antenna, the difference was 1.0 mm. For the ellipsoid height, the differences were 0.3 and 0.6 mm for the survey and Tallysman antennas, respectively. Comparison of low-cost receivers with low-cost survey calibrated antennas and geodetic instruments proved better performance for geodetic instruments. The geodetic GNSS instrument is more accurate than the low-cost instrument, and the precision of the coordinate estimation of the geodetic network is also greater. Low-cost GNSS instruments are not at the same level as geodetic instruments; however, considering their cost, they show excellent performance that is quite suitable for various geodetic applications.

The purpose of this research is to get a GNSS prototype that can produce raw coordinate position data with the average method of three GPS and connected and updated automatically, for precision ellipsoid height detection and to analyze the policy of an area that has certain ellipsoid contours as an object. This research is very important to use because GNSS refers to a constellation of satellites that provide positioning, navigation and timing services in real time. GNSS technology also as an innovation in the field of tracking devices offers many advantages that encourage efficiency and safety in tracking, the development of GNSS enabled satellites is needed as a precise, reliable, and flexible tracking in navigating the complexity of modern networks.

2. METHOD

In the research, an applied research approach will be carried out, namely as engineering research on the application of science into a tool design to obtain tool performance in accordance with specified requirements [8]. The design is a synthesis of design elements combined with scientific methods into a system that meets certain specifications [9]. The research design is i) determining the measurement accuracy

specifications of the tool into several design alternatives, ii) choosing one of the best design alternatives to be applied, and iii) assembling the module, namely the antenna bracket, the method of sending and retrieving data, the use of main and supporting materials and the level of data accuracy. The prototype design produces a GNSS system that can be used for ellipsoid height detection as shown in Figure 1.

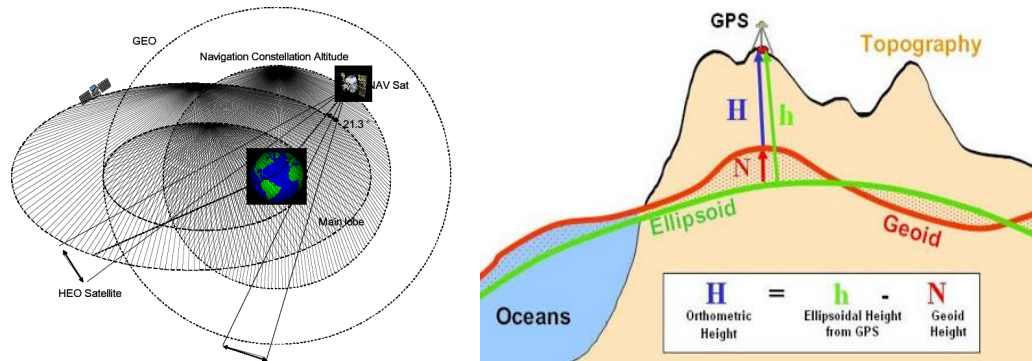


Figure 1. GNSS satellite orbits and illustrations of ellipsoid, geoid, and topographic positions

2.1. Global navigation satellite system

GNSS is a navigation system used to determine the position on the earth's surface [10], GNSS is a technology used to determine the position or location (latitude, longitude, and altitude) and time in scientific units on earth [11]. Satellites will transmit high-frequency radio signals containing time and position data that can be picked up by receivers that allow users to know the location anywhere on the earth's surface [12]. GNSS signals originating from satellites travel through the Earth's atmospheric layers, so the satellite signals experience delays, this affects the time it takes for the signal from the satellite to travel to the GNSS receiver, which has a slight error into the GNSS receiver, causing an error in the position measurement [13].

The first cause of delay is that the signal must travel through the ionosphere which is the outer edge of the atmosphere. The atmosphere is exposed to solar radiation which causes particles to become positively charged. This layer of the atmosphere has the greatest impact on passing electromagnetic signals that have radio signals sent from satellites. The influence of the ionosphere will add a relatively large delay depending on the location of the receiver, the location of the satellite, the time of day, the activity of the solar flare, from these factors it is concluded that the satellite's journey, experiences a delay of up to 16 newton seconds (16 NS). This can cause an error of up to 5 meters in the position taken [14].

The second delay is the signal from traveling through the troposphere, the weather part of the atmosphere, which includes conditions such as clouds, rain and lightning. This adds a much smaller delay to the signal of up to 1.5 NS, which can introduce position errors of up to 0.5 m. These delays are random delays that fluctuate so each individual satellite signal delay is positioned in a different area around the world, so the satellite signal will experience different atmospheric disturbances. The time delay from the satellite to the GNSS antenna can affect the recorded position data including the red circle which shows the error from the satellite indicated by atmospheric conditions [15].

2.2. Global positioning system

GPS is a satellite-based navigation system developed by the US Department of Defense (DoD) in the early 1970s. Initially, GPS was developed as a military system to meet the needs of the United States military. Soon after, however, access was made available to civilians and it is now a dual-system that can be accessed by both military and civilian users [16]. The system, which nominally consists of 24 satellites, can be used by many people at once in all weathers, and is designed to provide precise three-dimensional position and velocity as well as continuous time information around the world [17].

Basically, GPS consists of three main segments, namely the space segment consisting of GPS satellites equipped with antennas to receive and send wave signals, functioning as radio stations in space [18]. The control system segment consists of satellite monitoring and control stations that function to monitor and control the work of all satellites and ensure the functions of all satellites work well according to their functions and the user segment. In the user segment there are GPS receivers that are used to receive and process signals from GPS satellites to be used in determining position information, speed, time and other derived parameters [19].

Each GPS satellite continuously emits wave signals at two L-band frequencies called L1 and L2, the L1 signal has a frequency of 1575.42 MHz and the L2 signal has a frequency of 1227.60 MHz the L1 signal carries two binary codes called P-code (P-code, precise or private code) and C/A-code (C/A-code, clear access or coarse acquisition), while the L2 signal carries only C/A-code. It should be noted that at present the P-code has been converted into a Y-code whose structure is kept secret to the public [20]. Using the differential (relative) positioning method that uses a minimum of two GPS receivers' results in relatively higher positioning accuracy [21]. GPS can provide positions instantly (real-time) or after the observation after the observation data is processed more extensively (post processing) which is usually done to get better accuracy. The accuracy of GPS positions obtained from observations depends on four factors, namely i) positioning method, ii) geometry and distribution of the observed satellites, iii) data accuracy, and iv) data processing strategy/method, with GPS the point to be determined can be stationary (static positioning) or moving (kinematic positioning). The position of the point can be determined using one GPS receiver against the center of the earth using the absolute (point) positioning method, or against other points that have known coordinates [22].

2.3. Global positioning system errors and bias

There are several types of errors and biases that affect GPS observation data, including errors and biases related to satellites (such as ephemeris errors, satellite clocks, and selective availability), propagation medium (such as ionospheric bias and tropospheric bias), GPS receivers (such as receiver clock errors, antenna errors, and noise), observation data (phase ambiguity and cycle slips), and the environment around GPS receivers such as multipath [23]. GPS errors and biases must be properly and properly accounted for as they will affect the accuracy of the information (position, velocity, acceleration, time) obtained as well as the process of determining the phase ambiguity of the GPS signal. The observation strategy applied will also affect the effect of errors and biases on the observation data [24].

In addition, the structure and level of sophistication of the GPS data processing software will be affected by the mechanisms used to deal with errors and biases. A more detailed explanation of the effects of errors and biases. In general, there are several ways that can be used in dealing with errors, namely i) estimate the parameters of errors and biases in the process of calculating averaging, ii) apply a differencing mechanism between data, iii) calculate the amount of error/bias based on size data, iv) calculate the amount of error/bias based on the model, and v) use the right observation strategy, vi) use the right data processing strategy.

2.4. Height difference measurement

Measurement of height difference is a measurement work to determine the height difference of several points on the earth's surface against the average sea level, conceptually the height difference is defined as the difference between the two Nivo planes through two points on the earth's surface, the Nivo plane is an equipotential horizontal plane perpendicular to the gravity direction line through a point [25]. In measuring height, there are several terms that are often used i) a vertical line is a line that points to the center of the earth, which is generally considered the same as an endless line, ii) a horizontal plane is a plane perpendicular to the vertical line at each point. The horizontal plane is curved to follow the sea surface, iii) datum is a plane used as a reference plane for height, such as mean sea level, iv) elevation is the vertical distance (height) measured against the datum plane, and v) Banchmark is a fixed point whose elevation is known against the datum used, to guide the measurement of the elevation of the surrounding area [26].

The measurement of the height difference made by the flat sipat or water pass method is the most thorough method compared to other methods, the height of an object on the earth's surface is the height measured from a reference plane, whose height is considered zero [27]. The geodetic reference plane is called the geoid, which is an equipotential plane that coincides with the mean sea level, or also called the Nivo plane and these planes are always perpendicular to the direction of gravity towards each point on the earth's surface [28]. Using water pass equipment with a tripod, the difference in the center thread reading between the two rear signs less the face sign is used to determine the height difference between two points on the surface of the earth, measuring tape and meter, as well as the basic principle of measuring height with a water pass to measure the height difference between two points on the earth's surface. Flat-fold height difference measurement is still the most thorough way of measuring height difference to get the orthometric height of the ellipsoid height, other additional data is needed, namely geoid undulation [29]. With the undulation, the orthometric height can be calculated from the height of the ellipsoid and there are several methods to get the price of geoid undulation including the geometric method and the gravimetric method, in the geometric method, geoid undulation is calculated from a combination of satellite position height data with height and flat fold measurements. In the gravimetric method, geoid undulation is calculated from terrestrial gravity data and the global geopotential model [30].

2.5. Height determination with GPS

The height of the point given by GPS is the height of the point above the surface of the ellipsoid, namely the WGS84 ellipsoid, the ellipsoid height (h) is not the same as the orthometric height (H) obtained from the measurement of levelling, the orthometric height of a point is the height of the point above the geoid measured along the gravity line through the point [31]. The ellipsoid height of a point is the height of that point above the ellipsoid calculated along the ellipsoid normal line through that point for practical purposes the geoid is generally considered to coincide with mean sea level [32]. The geoid is a reference plane for expressing orthometric height, mathematically the geoid is a very complex surface that requires very many parameters to represent the earth mathematically and for mathematical calculations people generally use a reference ellipsoid and not a geoid [33]. The reference ellipsoid and geoid generally do not coincide, and in this case the height of the geoid with respect to the ellipsoid is called the geoid undulation (N), to be able to transform the ellipsoid height from the GPS measurement to the orthometric height, the geoid undulation at the corresponding point is required [34].

2.6. Monitoring land subsidence with GPS

GPS has been used successfully to observe the stability of structures, an application that requires high accuracy including deformation monitoring of dams, bridges and television towers. Monitoring subsidence of oil fields and mining areas is another example where GPS has been used successfully, monitoring subsidence by taking GPS measurements of the same area at different time intervals. Slow subsidence of structures such as dams requires millimeter accuracy to monitor subsidence.

With today's GPS satellites and GPS receivers, as well as mathematical alignment models, subsidence can be seen well enough for an informative subsidence analysis to be made [35]. Points placed at selected locations are periodically and carefully coordinated using the survey method studying the pattern and speed of coordinate changes of these points from one survey to the next. The subsidence characteristics can be calculated and further studied. Therefore, in the study of subsidence using GPS survey method, there are several advantages and benefits offered, as described in the following points [36].

The principle of monitoring land subsidence with GPS is to place monitoring points in several selected locations, carried out continuously so that the coordinates of the monitoring points can be determined carefully and from GPS observations the data to be obtained are in the form of monitoring point coordinates and time. By making periodic observations, changes in the position of a monitoring point can be identified by looking at changes in the coordinate value of the monitoring point from time to time. To get the value of land subsidence is to determine the height difference of each measurement [37].

2.7. Statistical data test

The standard deviation value is a value used in determining the distribution of data in a sample and seeing how close the data is to the mean value. Standard deviation or standard deviation is the best measure of spread, because it describes the magnitude of the spread of each unit of observation [38]. Standard deviation is the square root value of a variance which is used to assess the average or expected. Standard deviation or standard deviation of data that has been arranged in a frequency table.

The standard deviation value is a value used in determining the distribution of data in a sample and seeing how close the data is to the mean value [39]. Statistically, it is stated that the larger the sample size, the better the results. With a large sample, the mean and standard deviation obtained have a high probability of resembling the mean and standard deviation of the population. This is because the sample size is related to statistical hypothesis testing, although a large sample will be better, a small sample when randomly selected can also accurately reflect the population [40].

The standard deviation value is a value used in determining the distribution of data in a sample and seeing how close the data is to the mean value, the greater the standard deviation value, the more diverse the values on the item or the more inaccurate the mean, conversely the smaller the standard deviation, the more similar the values on the item or the more accurate the mean [41]. Analysis of calculations with the mean method, namely calculating the average value is to add up all individual data in the group, then divide by the number of individuals in the group, as in (1):

$$\text{Mean } X = \frac{\sum Xi}{n} = \frac{1}{n} (X1 + X2 + \dots + Xn) \quad (1)$$

where X is the mean or average, \sum is the sum, Xn is the variable and n is the number of values.

To calculate the median, the middle value is based on the middle value of the data group that has been arranged in order from smallest to largest or vice versa from largest to smallest, as in (2):

$$Median = \frac{X1+X2}{2} \tag{2}$$

where *Med* is the median, *X1* is the middle value where the median is located and *X2* the second middle value where the median is located.

To calculate the frequently occurring value from a group of data that has the highest frequency or the most occurring value in a group of values, as in (3):

$$Mo = TB + \frac{a}{(a+b)} \times C \tag{3}$$

where *Mo* is the mode, *TB* is the lower point of the mode class (the class with the largest frequency), *a* is the difference between the frequency of the *Mo* class and the previous one, *b* is the difference between the *Mo* frequency and the one after it and *c* is the class interval.

To calculate the standard deviation of individual values against the group mean, the standard deviation is the square root of the variance and indicates the standard deviation of the data from its mean value, as in (4):

$$S = \frac{\sqrt{\sum(X1-Xni)^2}}{n-1} \tag{4}$$

where *S* is the standard deviation, *N* is the number of data, *X1* is the 1st to nth *X* value and *x* is the average *x* value.

2.8. Prototype design

At the prototype design stage, the equipment needed is the u-blok Neo-7M module which functions to receive GNSS signals, these signals provide certain codes, so they can be recognized at the receiver. From GNNS then sends these codes to the Arduino Uno module and Arduino immediately performs the storage process on the SD Card. From GNNS, the data received to the ESP32 Wi-Fi module for further processing to the database server storage. The results of the design model can be seen in the design of Figure 2 which shows the general installation of the system to be made.

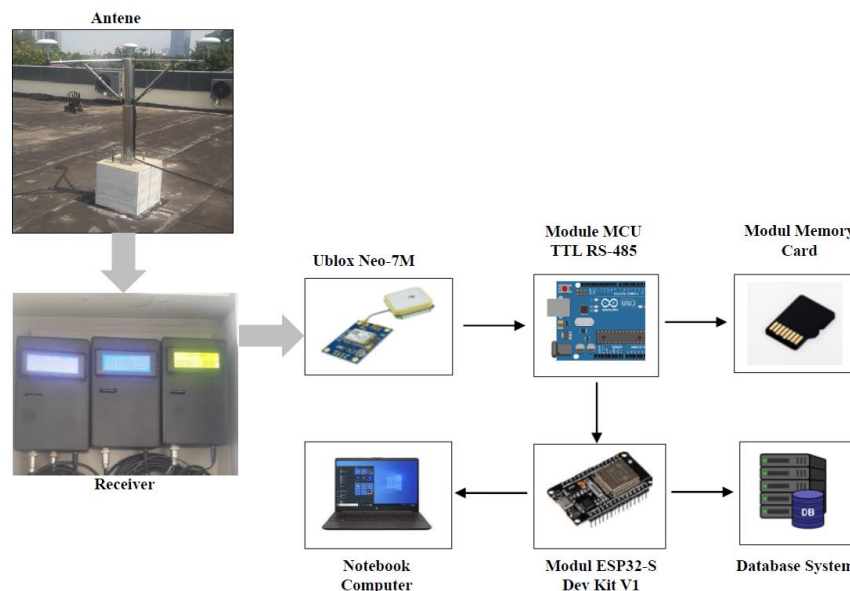


Figure 2. Prototype of GNSS system

The way the tool works is that the GPS antenna consists of a u-blok Neo-7M module which functions to find four or more satellites by detecting signals emitted from satellites received by the GPS antenna, then connected via an RS-485 module for further processing on the Arduino Uno module, then the received satellite signal will be sent to the receiver via a data cable. GPS receiver which functions to receive and store satellite signal data received by the GPS antenna and send the data to the web server system

consisting of Arduino Uno components connected via RS-485 module to program the SSD card module as data storage and program the Esp32-S Wi-Fi module for the process of sending data to the web server system in real time. The poles used use 304 stainless steel-based pipes which have anti-corrosion properties and have better strength in outdoor with sizes of 4 inches and 1 inch with a pole height of 120 cm and the length of each side is 60 cm, in assembling this pole using the equilateral triangle method and also requires accuracy so that no errors occur when welding.

3. RESULTS AND DISCUSSION

In the design and assembly of this web-based GNSS continues positioning system prototype is divided into three parts, namely i) the GPS antenna functions to detect and receive electromagnetic waves emitted by GNSS satellites then sent to the receiver for further processing; ii) the receiver functions to process the data received by the GPS antenna, then the data is stored in the memory card module, and sends the data to the base server; and iii) the website functions to display the page or data information received by the receiver to be presented to the user in order to facilitate the process of downloading and processing data. In the design and assembly of this GNSS system prototype, several equipment is used as support, namely antennas, receivers and web information. Basically, the method in determining the position using GNSS can be grouped into several modes that can be used based on the needs of kinematic, static, rapid static, pseudo-kinematic stop and go. In this study the method used is pseudo-kinematic stop and go so that the accuracy used is precision. the difference with GNSS with navigation satellites is that it has the ability to provide information related to the position of the location geographically and time synchronization in the use of signal in real time from navigation satellites orbiting in the sky, navigation satellites are generally used in various sectors such as research accuracy, support in search and rescue, earth science, transportation.

3.1. GNSS observation training data with absolute method

Observations were carried out for one hour with an observation time interval of one second with the observation location at XYZ, with coordinates 06°09'49.59153 "S - 106°53'07.97377 "E. Then the observation data was downloaded and the data was validated using raw conversion from decimal degrees format to UTM (coordinated universal time) format. Furthermore, to analyze and find out how big the standard deviation is, an analysis is carried out using a statistical formula. This is done to find out and ascertain whether this tool can really record raw from GNSS signal recording results, as well as to find out the quality of the data can be validated correctly. The observation distribution data used is 3,600 data received at the GPS receiver, the observation results of the distribution data will be used as training data, as in Table 1.

Table 1. Raw distribution of observations from GPS receivers

No	Date	Times	Coordinate					
			GPS-1		GPS-2		GPS-3	
			Easting	Northing	Easting	Northing	Easting	Northing
1	05/11/2023	10:29:00	708643.608	10681677.855	708651.688	10681678.234	708647.721	10681678.312
2	05/11/2023	10:29:01	708643.590	10681677.855	708651.706	10681678.215	708647.739	10681678.367
3	05/11/2023	10:29:02	708643.590	10681677.836	708651.688	10681678.123	708647.776	10681678.386
4	05/11/2023	10:29:03	708643.571	10681677.818	708651.670	10681678.031	708647.813	10681678.423
5	05/11/2023	10:29:04	708643.553	10681677.818	708651.670	10681678.086	708647.831	10681678.441
...
3599	05/11/2023	11:28:58	708646.405	10681680.058	708647.481	10681683.436	708646.729	10681676.981
3600	05/11/2023	11:28:59	708646.386	10681680.040	708647.463	10681683.436	708646.766	10681676.963

To obtain valid data from GPS-1, GPS-2, GPS-2 after conversion to UTM, the observation data is analyzed using a statistical formula equation with the absolute method (mean, median, mode, standard deviation) with the formula (1):

$$\text{Mean } X = \frac{\sum Xi}{n} = \frac{1}{n} (X1 + X2 + \dots + Xn) \quad (1)$$

GPS-1

Easting : 708646.96
 Northing : 10681678.66

GPS-2

Easting : 708649.53
 Northing : 10681679.41

GPS-3

Easting : 708645.99
 Northing : 10681678.08

$$\text{Median } (Me = \frac{x_1+x_2}{2}) \tag{2}$$

GPS-1

Easting : 708646.88
 Northing : 10681678.80

GPS-2

Easting : 708649.46
 Northing : 10681679.64

GPS-3

Easting : 708646.03
 Northing : 10681678.10

$$\text{Modus } (Mo = TB + \frac{a}{(a+b)} xC) \tag{3}$$

GPS-1

Easting : 708646.58
 Northing : 1010681678.44

GPS-2

Easting : 708649.58
 Northing : 10681679.30

GPS-3

Easting : 708645.99
 Northing : 10681677.88

$$\text{Standard Deviation } (S = \frac{\sqrt{\sum(X_1-x_{ni})^2}}{n-1}) \tag{4}$$

GPS-1

Easting : 1.09
 Northing : 1.08

GPS-2

Easting : 1.19
 Northing : 1.32

GPS-3

Easting : 0.54
 Northing : 0.64

Details of the recapitulation of calculations using statistical formula equations with absolute methods (mean, median, mode, standard deviation) can be seen in Table 2. For the calculation of standard deviation on GPS-1 easting of 1.09 m and northing of 1.08 m, GPS-2 easting of 1.19 m and northing of 1.32 m, GPS-3 easting of 0.54 m and northing of 0.64 m. Circular error probability (CEP) standardization issued by u-blox Neo 7M from the calculation results has met the standard of 2.5 m.

Furthermore, to analyze and find out how big the standard deviation is on the training data, the observation results will be analyzed using statistical formulas. With observation is on the distribution data of 3,600 data received at the GPS receiver. The results of the observation analysis of the distribution data will be used as training data to obtain real data. Distribution data of raw observations on global positioning system as shown in Table 3.

Table 2. Recapitulation of GPS observation data calculation results

Test with equation formulas		GPS-1		GPS-2		GPS-3	
		Easting	Northing	Easting	Northing	Easting	Northing
Mean (X)	(1)	708646.96	10681678.66	708649.53	10681679.41	708645.99	10681678.08
Median (Me)	(2)	708646.88	10681678.80	708649.46	10681679.64	708646.03	10681678.10
Modus (Mo)	(3)	708646.58	10681678.44	708649.58	10681679.30	708645.99	10681677.88
Standard Deviation (S)	(4)	1.09	1.08	1.19	1.32	0.54	0.64

Table 3. Raw distribution of observations from GPS receivers

No	Date	Clock	GPS-AVG		GPS TRIMBLE-8	
			Easting	Northing	Easting	Northing
1	05/11/2023	10:29:00	708647.666	10681678.127	708647.288	10681679.009
2	05/11/2023	10:29:01	708647.666	10681678.146	708647.288	10681679.009
3	05/11/2023	10:29:02	708647.685	10681678.109	708647.288	10681679.009
4	05/11/2023	10:29:03	708647.685	10681678.091	708647.288	10681679.009
5	05/11/2023	10:29:04	708647.685	10681678.109	708647.288	10681679.009
...
3599	05/11/2023	11:28:58	708646.679	10681680.723	708646.679	10681680.723
3600	05/11/2023	11:28:59	708646.661	10681680.723	708646.661	10681680.723

Calculation of data from GPS-AVG and Trimble-8 GPS with valid after conversion to UTM, then the observation data is analyzed using statistical formula equations with absolute methods (mean, median, mode, standard deviation) with the following details:

$$\text{Mean } X = \frac{\sum X_i}{n} = \frac{1}{n} (X_1 + X_2 + \dots + X_n) \quad (5)$$

GPS-AVG

Easting : 708647.53
 Northing : 10681678.72

GPS-TRIMBLE 8

Easting : 708647.27
 Northing : 10681679.30

$$\text{Median } (Me = \frac{X_1 + X_2}{2}) \quad (6)$$

GPS-AVG

Easting : 708647.46
 Northing : 10681678.79

GPS-TRIMBLE 8

Easting : 708647.25
 Northing : 10681679.29

$$\text{Modus } (Mo = TB + \frac{a}{(a+b)} xC) \quad (7)$$

GPS-AVG

Easting : 708646.87
 Northing : 10681678.64

GPS-TRIMBLE 8

Easting : 708647.29
 Northing : 10681679.33

$$\text{Standard Deviation } (S = \frac{\sqrt{\sum (X_1 - \bar{X}_n)^2}}{n-1}) \quad (8)$$

GPS-AVG

Easting : 0.56
 Northing : 0.64

GPS-TRIMBLE 8

Easting : 0.14
 Northing : 0.27

Details of the recapitulation of calculations using statistical formula equations with absolute methods (mean, median, mode, standard deviation) can be seen in Table 4. For the calculation of standard deviation on GPS-AVG easting of 0.56 m and northing of 0.27 m, GPS-TRIMBLE R8 easting of 0.14 m and northing of 0.27 m. Circular error probability (CEP) standardization issued by u-blox Neo 7M from the calculation results has met the standard of 2.5 m. Visualization of the analysis of the results of the comparison of the standard deviation of easting and northing coordinates on each GPS-AVG and GPS-Trimble R8 as shown in Figure 3.

Table 4. Recapitulation result of GPS observation data calculation

Test with equation formulas	GPS-AVG		GPS-TRIMBLE R8	
	Easting	Northing	Easting	Northing
Mean (<i>X</i>)	708647.53	10681678.72	708647.27	10681679.30
Median (<i>Me</i>)	708647.46	10681678.79	708647.25	10681679.29
Modus (<i>Mo</i>)	708646.87	10681678.64	708647.29	10681679.33
Standard Deviation (<i>S</i>)	0.56	0.64	0.14	0.27

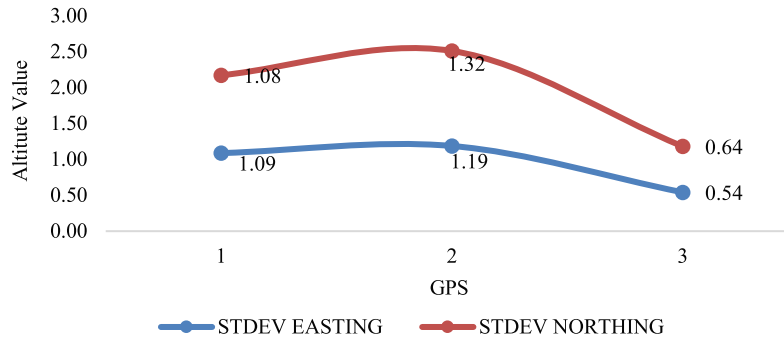


Figure 3. Visualization of standard deviation comparison for each GPS

3.2. Training data of altitude observation with absolute method

Altitude observations were carried out for fifteen days from November 05, 2023 to November 20, 2023 with an observation time interval of fifteen minutes, with the observation location at XYZ, with coordinates 06°09'49.59153 "S - 106°53'07.97377 "E. Then the observation data was downloaded and the data was validated using raw conversion from decimal degrees format to coordinated universal time (UTM) format. Furthermore, to analyze and find out how big the standard deviation is, an analysis is carried out using the statistical equation formula. This is done to find out and ascertain whether this tool can really record raw from GNSS signal recording results, and to find out the quality of the data can be validated correctly. The height observation distribution data used is 1,536 data received at the GPS receiver, the height observation results from the distribution data will be used as training data, as shown in Table 5.

Table 5. GPS elevation distribution training data

No.	Date	Times	Training data distributing altitude								
			MSL altitude			GEOID separation			HIGH ellipsoid		
			GPS-1	GPS-2	GPS-3	GPS-1	GPS-2	GPS-3	GPS-1	GPS-2	GPS-3
1	05/11/2023	00:00	29.80	32.90	33.30	2.10	2.10	30.80	27.70	30.80	31.20
2	05/11/2023	00:15	33.40	33.70	32.40	2.10	2.10	31.60	31.30	31.60	30.30
3	05/11/2023	00:30	33.30	28.60	34.90	2.10	2.10	26.50	31.20	26.50	32.80
4	05/11/2023	00:45	34.20	30.70	31.30	2.10	2.10	28.60	32.10	28.60	29.20
5	05/11/2023	01:00	26.90	31.00	29.10	2.10	2.10	28.90	24.80	28.90	27.00
...
1535	20/11/2023	23:30	27.10	32.50	29.00	2.10	2.10	30.40	25.00	30.40	26.90
1536	20/11/2023	23:45	27.20	30.40	30.20	2.10	2.10	28.30	25.10	28.30	28.10

To obtain valid altitude data from the GPS receiver with HIGH Ellipsoid after conversion to UTM, the observation data is analyzed using a statistical formula equation with the absolute method (mean, median, mode, standard deviation) with the formula:

$$\text{Mean } (X = \frac{\sum Xi}{n} = \frac{1}{n} (X1 + X2 + \dots + Xn)) \tag{9}$$

GPS-1 : 26.30
 GPS-2 : 26.50
 GPS-3 : 26.90

$$\text{Median } (Me = \frac{X1+X2}{2}) \tag{10}$$

GPS-1 : 26.38
 GPS-2 : 25.94
 GPS-3 : 27.13

$$\text{Modus } (Mo = TB + \frac{a}{(a+b)} xC) \tag{11}$$

GPS-1 : 28.20
 GPS-2 : 28.60
 GPS-3 : 25.80

$$\text{Standard Deviation } (S = \frac{\sqrt{\sum(X1-Xni)^2}}{n-1}) \tag{12}$$

GPS-1 : 3.75
 GPS-2 : 4.28
 GPS-3 : 3.69

Details of the recapitulation of calculations using statistical formula equations with absolute methods (mean, median, mode, standard deviation) can be seen in Table 6. For the calculation of standard deviation on the HIGH Ellipsoid is GPS-1 of 3.76 m, GPS-2 of 4.28 m and GPS-3 of 3.69m. Visualization of the analysis of the results of the comparison of standard deviation of coordinates on each GPS-1, GPS-2, GPS-3 as in Figure 4.

Table 6. Results of recapitulation of HIGH Ellipsoid altitude data calculation

Test with equation formulas	HIGH Ellipsoid		
	GPS-1	GPS-2	GPS-3
Mean (<i>X</i>)	26.30	26.50	26.90
Median (<i>Me</i>)	26.38	25.94	27.13
Modus (<i>Mo</i>)	28.20	28.60	25.80
Standard Deviation (<i>S</i>)	3.76	4.28	3.69

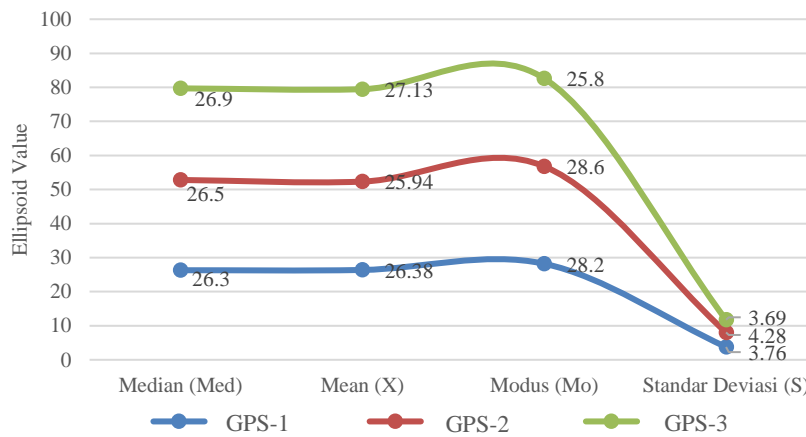


Figure 4. Standard deviation comparison visualization graph for each GPS

3.3. Plot of raw GPS observation and correction

Observations were carried out for one hour with an observation time interval of one second, using the data comparison method using the GPS-Trimble R8 device at the same point. The observation location at XYZ at coordinates 06° 09'49.59153 "S - 106° 53'07.97377 "E. Then the observation data is downloaded and the data is validated using raw conversion from decimal degrees format to UTM format. Furthermore, to analyze and find out how much the observation data is downloaded and then the data is validated to find out how much accuracy of the GNSS continuous positioning system prototype tool. This is done to find out and make sure, whether this tool can really record raw from GPS observations and to find out the quality of the data can be validated, the results of the analysis as in Figure 5.

From the analysis of Figure 5 that the results of the GPS raw data plot are obtained for green warrants are raw data from GPS-Trimble R8, blue is GPS-1 raw data, orange is GPS-2 raw data, yellow is GPS-3 raw data, purple is GPS-AVG raw data. The results of averaging the three raw data from GPS-1, GPS-2 and GPS-3 with a simple smoothing method, resulting in that the distribution accuracy of the prototype tool can be in the distribution position of the GPS-Trimble R8 tool. From the results of the analysis of Figure 5 that the results of the GPS raw data plot obtained for green warrants are raw data from GPS-Trimble R8, blue is GPS-1 raw data, orange is GPS-2 raw data, yellow is GPS-3 raw data, purple is GPS-AVG raw data.

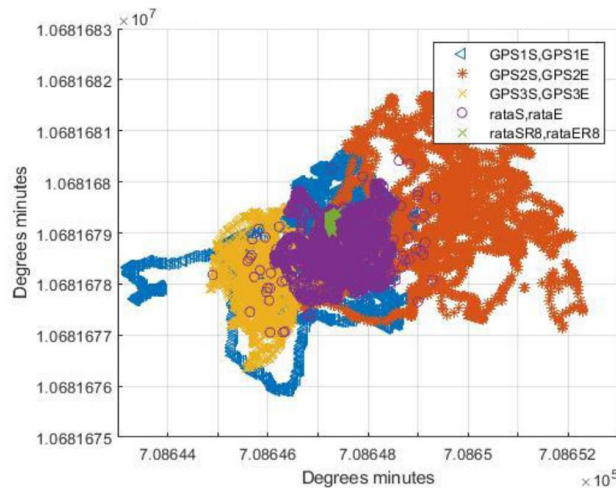


Figure 5. GPS row plot results and correction results

3.4. Plot of raw altitude and its correction results

Altitude observations were carried out for fifteen days from November 05, 2023 to November 20, 2023 with an observation time interval of fifteen minutes, with the observation location at XYZ, with coordinates 06 09'49.59153 "S - 106 53'07.97377 "E. Then the observation data was downloaded and the data was validated using raw conversion from decimal degrees format to UTM format. Furthermore, to analyze and find out how much accuracy of the GNSS continuous positioning system prototype tool. This is done in order to know and ensure, whether this tool can actually record raw data from the GNSS signal recording results and to determine the quality of the data can be validated, the results of the analysis as shown in Figure 6.

From the analysis of Figure 6 that the results of the altitude raw data plot can be analyzed for orange color is raw data from GPS-1, yellow color is GPS-2 raw data, green color is GPS-3 raw data and brown color is GPS-AVG raw data or the average result of the three raw data from GPS-1, GPS-2 and GPS-3. With the simple smoothing method and the least square method, it is found that the altitude accuracy of the prototype is at an altitude position of 28.7 meters from the ellipsoid height obtained from the average value of the three GPS plus the height of the GPS antenna.

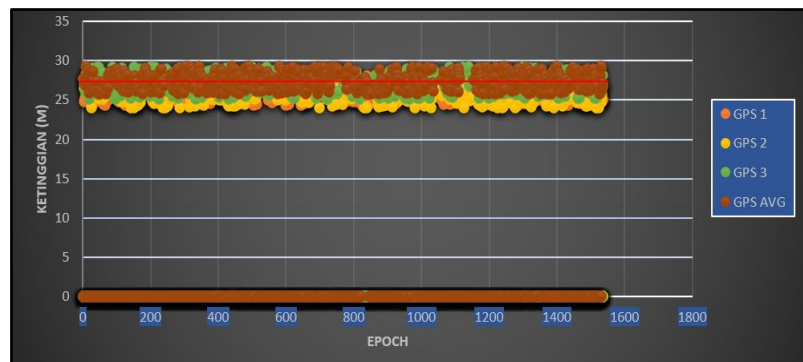


Figure 6. Results of raw height plot and its correction

4. CONCLUSION

The purpose of this research is to obtain a prototype GNSS system that can produce raw GPS position data. By averaging three methods GPS-1, GPS-2 and GPS-3 can be used for the detection of ellipsoid height at the object location. Data processing with observation results can be obtained prototype GNSS continuous positioning system can be programmed to produce raw data position data. With a precise level of accuracy using a simple averaging method that can be programmed in order to produce raw height data for ellipsoid height detection in certain areas.

The results of this study are with the observation of the absolute method for one hour, the results of validation of position accuracy data for i) GPS-1 easting of 1.09 m and northing of 1.08 m, ii) GPS-2 easting of 1.19 m and northing of 1.32 m and iii) GPS-3 easting of 0.54 m and northing of 0.64 m. GPS-AVG or the average of the three GPS obtained easting of 0.56 m and northing of 0.64 m, GPS-AVG or the average of the three GPS obtained easting of 0.56 m and northing of 0.64 m, 56 m and northing of 0.64 m. While raw altitude data obtained standard deviation data of 0.56 m and 0.64 m.

The raw altitude data obtained standard deviation data from GPS-1 of 3.76 m, GPS-2 of 4.26 m, GPS-3 of 3.69 m and GPS-AVG or the average of the three GPS obtained 3.01 m from the height of the ellipsoid. To produce a higher level of precision and accuracy, the u-blox 7M chip is replaced with other chip type specifications so as to get higher position accuracy results as well and the use of a data filtering system in the Arduino programming system, so that the results of the ellipsoid height in the XYZ area are better expected to make continuous observations.




REFERENCES

- [1] M. Haley, M. Ahmed, E. Gebremichael, D. Murgulet, and M. Starek, "Land subsidence in the Texas coastal bend: locations, rates, triggers, and consequences," *Remote Sensing*, vol. 14, no. 1, 2022, doi: 10.3390/rs14010192.
- [2] T. M. Roberts, T. K. Meehan, J. Y. Tien, and L. E. Young, "Detection and localization of terrestrial 1-band RFI with GNSS receivers," *IEEE Transactions on Geoscience and Remote Sensing*, vol. 60, 2022, doi: 10.1109/TGRS.2021.3109524.
- [3] A. Nowak, R. Zajdel, and K. Sośnica, "Optimization of orbit prediction strategies for GNSS satellites," *Acta Astronautica*, vol. 209, pp. 132–145, 2023, doi: 10.1016/j.actaastro.2023.04.040.
- [4] D. Sh. Akhmedov, N. B. Boguspaev, A. S. Raskaliev, A. I. Samsonenko, and S. Zh. Zhumagali, "Development of a simulation model for determining the coordinates of air objects based on the GNSS navigation signal reflected from the air object and received on the antenna of the navigation receiver," *Engineering Journal of Satbayev University*, vol. 145, no. 1, pp. 32–38, 2023, doi: 10.51301/ejsu.2023.i1.05.
- [5] A. Capelli *et al.*, "GNSS signal-based snow water equivalent determination for different snowpack conditions along a steep elevation gradient," *Cryosphere*, vol. 16, no. 2, pp. 505–531, 2022, doi: 10.5194/tc-16-505-2022.
- [6] A. Fedorchuk, "The potential application of the GNSS leveling method in local areas by means of sector analysis," *Geomatics and Environmental Engineering*, vol. 16, no. 3, pp. 41–55, 2022, doi: 10.7494/geom.2022.16.3.41.
- [7] V. Hamza, B. Stopar, and O. Sterle, "Testing the performance of multi-frequency low-cost gnss receivers and antennas," *Sensors*, vol. 21, no. 6, pp. 1–16, 2021, doi: 10.3390/s21062029.
- [8] L. Zhu, H. Zhang, X. Li, F. Zhu, and Y. Liu, "GNSS timing performance assessment and results analysis," *Sensors*, vol. 22, no. 7, 2022, doi: 10.3390/s22072486.
- [9] J. Dong, "A novel design of flat-top beamforming anti-multipath antenna," *Wireless Communications and Mobile Computing*, vol. 2022, 2022, doi: 10.1155/2022/9938813.
- [10] M. Rybansky *et al.*, "GNSS signal quality in forest stands for off-road vehicle navigation," *Applied Sciences (Switzerland)*, vol. 13, no. 10, 2023, doi: 10.3390/app13106142.
- [11] D. Egea-Roca *et al.*, "GNSS user technology: state-of-the-art and future trends," *IEEE Access*, vol. 10, pp. 39939–39968, 2022, doi: 10.1109/ACCESS.2022.3165594.
- [12] Y. Guo, Y. Rao, X. Wang, D. Zou, H. Shi, and N. Ji, "Carrier characteristic bias estimation between GNSS signals and its calibration in high-precision joint positioning," *Remote Sensing*, vol. 15, no. 4, 2023, doi: 10.3390/rs15041051.
- [13] D. Janos, P. Kuras, and L. Ortyl, "Evaluation of low-cost RTK GNSS receiver in motion under demanding conditions," *Measurement: Journal of the International Measurement Confederation*, vol. 201, 2022, doi: 10.1016/j.measurement.2022.111647.
- [14] B. Breitsch and Y. J. Morton, "A batch algorithm for GNSS carrier phase cycle slip correction," *IEEE Transactions on Geoscience and Remote Sensing*, vol. 60, 2022, doi: 10.1109/TGRS.2022.3151416.
- [15] X. Xia, E. Hashemi, L. Xiong, and A. Khajepour, "Autonomous vehicle kinematics and dynamics synthesis for sideslip angle estimation based on consensus Kalman filter," *IEEE Transactions on Control Systems Technology*, vol. 31, no. 1, pp. 179–192, 2023, doi: 10.1109/TCST.2022.3174511.
- [16] S. Bhamidipati, T. Mina, and G. Gao, "Time transfer from GPS for designing a SmallSat-based lunar navigation satellite system," *Navigation, Journal of the Institute of Navigation*, vol. 69, no. 3, 2022, doi: 10.33012/navi.535.
- [17] A. Lenczuk, A. Klos, and J. Bogusz, "Studying spatio-temporal patterns of vertical displacements caused by groundwater mass changes observed with GPS," *Remote Sensing of Environment*, vol. 292, 2023, doi: 10.1016/j.rse.2023.113597.
- [18] H. B. Lee, K. H. Kwon, and J. H. Won, "Feasibility analysis of GPS L2C signals for SSV receivers on SBAS GEO satellites," *Remote Sensing*, vol. 14, no. 21, 2022, doi: 10.3390/rs14215329.
- [19] Z. Rui, X. Ouyang, F. Zeng, and X. Xu, "Blind estimation of GPS M-code signals under noncooperative conditions," *Wireless Communications and Mobile Computing*, vol. 2022, 2022, doi: 10.1155/2022/6597297.
- [20] K. M. Abdel Aziz and L. Elsonbaty, "Effect of using different satellite ephemerides on GPS PPP and post processing techniques," *Geodesy and Cartography (Vilnius)*, vol. 47, no. 3, pp. 104–110, 2021, doi: 10.3846/gac.2021.13762.
- [21] Y. Qamaz, A. Schwering, and J. Biströn, "Experimental evaluation of using BLE beacon for outdoor positioning in GPS-denied environment," *AGILE: GIScience Series*, vol. 3, pp. 1–9, 2022, doi: 10.5194/agile-giss-3-13-2022.
- [22] A. Asraf, R. H. Surayuda, A. Z. Ribah, Kamirul, and M. Mukhayadi, "Determination of mean orbital elements using GPS data for LAPAN satellite daily operation," in *Proceedings of the 2021 IEEE International Conference on Aerospace Electronics and*




- Remote Sensing Technology, ICARES 2021*, 2021, pp. 1–6, doi: 10.1109/ICARES53960.2021.9665177.
- [23] J. Hong *et al.*, “Analysis of dual-frequency solution method for single-frequency precise point positioning based on SEID model for GPS and BDS,” *Measurement: Journal of the International Measurement Confederation*, vol. 175, 2021, doi: 10.1016/j.measurement.2021.109102.
- [24] A. Wageeh, M. Doma, A. Sedeek, and A. Elghazouly, “DCB estimation and analysis using the single receiver GPS/GLONASS observations under various seasons and geomagnetic activities,” *Advances in Space Research*, vol. 72, no. 9, pp. 3933–3945, 2023, doi: 10.1016/j.asr.2023.07.063.
- [25] O. Odalovic, K. Medved, and S. Naod, “Modeling of vertical gravity gradient by normal gravity field and digital terrain models,” *Journal of Geodesy*, vol. 96, no. 10, 2022, doi: 10.1007/s00190-022-01669-y.
- [26] G. Huang, S. Du, and D. Wang, “GNSS techniques for real-time monitoring of landslides: a review,” *Satellite Navigation*, vol. 4, no. 1, 2023, doi: 10.1186/s43020-023-00095-5.
- [27] K. Ansari, H. W. Seok, and P. Jamjareegulgarn, “Quasi zenith satellite system-reflectometry for sea-level measurement and implication of machine learning methodology,” *Scientific Reports*, vol. 12, no. 1, 2022, doi: 10.1038/s41598-022-25994-6.
- [28] M. Brach, “Rapid static positioning using a four system GNSS receivers in the forest environment,” *Forests*, vol. 13, no. 1, 2022, doi: 10.3390/f13010045.
- [29] H. Tata and R. Olatunji, “Determination of orthometric height using GNSS and EGM data: a scenario of the Federal University of Technology Akure,” *International Journal of Environment and Geoinformatics*, vol. 8, no. 1, pp. 100–105, 2021, doi: 10.30897/ijegeo.754808.
- [30] I. O. Raufu and H. Tata, “Comparison of two corrector surface models of orthometric heights from GPS/levelling observations and global gravity model,” *JGISE: Journal of Geospatial Information Science and Engineering*, vol. 5, no. 1, p. 15, 2022, doi: 10.22146/jgise.72531.
- [31] T. Herbert and E. S. Okiemute, “Determination of orthometric heights of points using gravimetric/GPS and geodetic levelling approaches,” *Indian Journal of Engineering*, vol. 18, no. 49, pp. 134–144, 2021, doi: 10.30897/ijegeo.899062.
- [32] W. H. F. Smith, “Direct conversion of latitude and height from one ellipsoid to another,” *Journal of Geodesy*, vol. 96, no. 5, 2022, doi: 10.1007/s00190-022-01608-x.
- [33] M. El-Diasty, M. R. Kaloop, and F. Alsaq, “Chart datum-to-ellipsoid separation model development for obhur creek using multibeam hydrographic surveying,” *Journal of Marine Science and Engineering*, vol. 10, no. 2, 2022, doi: 10.3390/jmse10020264.
- [34] M. Bergé-Nguyen *et al.*, “Mapping mean lake surface from satellite altimetry and GPS kinematic surveys,” *Advances in Space Research*, vol. 67, no. 3, pp. 985–1001, 2021, doi: 10.1016/j.asr.2020.11.001.
- [35] A. N. Safi’i, Susilo, D. Ramdani, and B. Muslim, “Utilization of Indonesia’s regional ionosphere model to improve the accuracy of GPS measurements to support disaster mitigation studies,” *IOP Conference Series: Earth and Environmental Science*, vol. 950, no. 1, 2022, doi: 10.1088/1755-1315/950/1/012097.
- [36] N. K. Ghazal and N. S. L. Saray, “A comparison of orthometric heights calculated from (GPS/Leveling) and (EGM08) methods based-GIS,” *Journal of Physics: Conference Series*, vol. 1879, no. 3, 2021, doi: 10.1088/1742-6596/1879/3/032072.
- [37] S. Ganguly and U. Bhan, “Remote sensing and GIS based monitoring and management of coastal aquifers and ecosystem,” *Springer Water*, vol. Part F1186, pp. 171–193, 2023, doi: 10.1007/978-3-031-35279-9_8.
- [38] M. Specht, “Consistency analysis of global positioning system position errors with typical statistical distributions,” *Journal of Navigation*, vol. 74, no. 6, pp. 1201–1218, 2021, doi: 10.1017/S0373463321000485.
- [39] N. Yilmaz, “Assessment of latest global gravity field models by GNSS/Levelling Geoid,” *International Journal of Engineering and Geosciences*, vol. 8, no. 2, pp. 111–118, 2023, doi: 10.26833/ijeg.1070042.
- [40] A. Rustamov, A. Minetto, and F. Dovis, “Improving GNSS spoofing awareness in smartphones via statistical processing of raw measurements,” *IEEE Open Journal of the Communications Society*, vol. 4, pp. 873–891, 2023, doi: 10.1109/OJCOMS.2023.3260905.
- [41] M. E. Elsobeiey, “Accuracy assessment of satellite-based correction service and virtual GNSS reference station for hydrographic surveying,” *Journal of Marine Science and Engineering*, vol. 8, no. 7, 2020, doi: 10.3390/JMSE8070542.

BIOGRAPHIES OF AUTHORS






Dwi Aji Zulfikar    graduated from Diploma III (A.Md). D-III Hydro-Oceanography Study Program at the Naval College of Technology 2024. He is currently active as a member in the Hydrographic and Oceanographic Center of the Navy. Research in the field of hydrography. He can be reached by email: dwiaji117@gmail.com.






Yoyok Nurkarya    Graduated from masters in geodesy and geomatics engineering (M.T). Geodesy and Geomatics Engineering at the Bandung Institute of Technology in 2007. Currently active as a lecturer at the Indonesian Naval Technology College. Research in the field of hydrography and surveying. He can be contacted at email: ynksantosa@gmail.com.






Johar Setiyadi    graduated from masters in geodesy and geomatics engineering (M.T). Geodesy and Geomatics Engineering, Bandung Institute of Technology in 2007. Currently active as a lecturer at the Indonesian Naval Technology College. Research in the fields of hydrography, maritime meteorology, land subsidence. He can be contacted at email: jsetiyadi99@gmail.com.






Endro Sigit Kurniawan    graduated from masters in geodesy and geomatics engineering (M.T). Geodesy and Geomatics Engineering at the Bandung Institute of Technology in 2016. Currently active as a lecturer at the Indonesian Naval Technology College. Research in the field of hydrography and surveying. He can be contacted at email: endro.sigit03@gmail.com.



Carudin    graduated from masters in computer science (M.Kom) at Budi Luhur University Jakarta Information Systems Study Program in 2019. Currently he is active as a lecturer in the Information Management Department, Faculty of Information and Digital Technology, Bani Saleh University, Bekasi, Indonesia. Research in the field of software engineering and internet of things. He can be contacted at email: carudin2905@gmail.com.



Suhadi    graduated from master of informatics engineering (M.Kom), at the Informatics Engineering Study Program, Eresha College of Informatics and Computer Management, Jakarta in 2011. Worked as a State Civil Apparatus (ASN) at the Directorate General of Capture Fisheries, Ministry of Marine Affairs and Fisheries Republic of Indonesia. Since 2016 until now he has been active as a lecturer in the Informatics Engineering Study Program, Faculty of Information and Digital Technology, Bani Saleh University, Bekasi-Indonesia. Research interests in software engineering, data mining, intelligent systems, and digital forensics. He can be contacted at email: hadims71ndl@gmail.com.